ANADOLU ÜNİVERSİTESİ BİLİM VE TEKNOLOJİ DERGİSİ
ANADOLU UNIVERSITY JOURNAL OF SCIENCE AND TECHNOLOGY
Cilt/Vol.:8-Sayı/No: 1 : 247-253 (2007)

RESEARCH ARTICLE/**ARAŞTIRMA MAKALESİ**

LEVEL DENSITIES AND RADIATIVE STRENGTH FUNCTIONS IN ^{56,57}Fe AND ^{96,97}Mo

E. Algin[1], A. Schiller[2], A. Voinov[3], U. Agvaanluvsan[4], T. Belgya[5], L.A. Bernstein[2], R. Chankova[6], P.E. Garrett[2], M. Guttormsen[6], M. Hjorth-Jensen[6], C. W. Johnson[7], G.E. Mitchell[4], J. Rekstad[6], S. Siem[6], W. Younes[2]

ABSTRACT

Nuclear level densities and radiative strength functions (RSFs) are measured for ^{56,57}Fe and ^{96,97}Mo isotopes using a light ion reaction. Observed step structure in the level density curves is explained tentatively by a schematic microscopic model implemented with seniority-conserving and seniority-nonconserving interactions. An unusual strong enhancement of the soft ($E_\gamma \leq 2$ MeV) radiative strength function for transitions in the quasicontinuum is observed in these isotopes. Experimental two-step cascade intensities with soft primary transitions from the ^{56}Fe(n,2γ)^{57}Fe reaction confirm the enhancement.

Keywords : Nuclear level densities, Radiative strength functions.

^{56,57}Fe VE ^{96,97}Mo ÇEKİRDEKLERİNDE ENERJİ DURUM YOĞUNLUKLARI VE GAMA IŞINI KUVVET FONKSİYONLARI

ÖZ

^{56,57}Fe ve ^{96,97}Mo izotoplarının nükleer durum yoğunluğu ve gama kuvvet fonksiyonu hafif-iyon reaksiyonu kullanılarak ölçülmüştür. Durum yoğunluğu eğrilerinde gözlenen merdiven yapısı, sinyorite-korunumlu ve sinyorite-korunumsuz etkileşmeleri içeren bir şematik mikroskopik model ile açıklanmıştır. Bu izotoplarda yirast eğrisinin birçok MeV üzerinden gelen gama geçişlerinde, gama kuvvet fonksiyonlarının düşük enerjili gamalar için çok yüksek olduğu gözlenmiştir. ^{56}Fe(n,2γ) ^{57}Fe reaksiyonunu kullanan iki-adım gama geçişi deneyi, düşük enerjili gama ışınlarının daha büyük şiddetle yayınlandığını doğrulamaktadır.

Anahtar Kelimeler: Nükleer enerji durumları yoğunlukları, Gama-ışını kuvvet fonksiyonları.

[1] Department of Physics, Eskisehir Osmangazi University, Eskisehir 26480 Turkey
fax: 0 222 239 3578, **e-mail:** tavukcu@ogu.edu.tr
[2] Lawrence Livermore National Laboratory,L-414, 7000 East Avenue, Livermore, CA 94551, USA
[3] Department of Physics and Astronomy, Ohio University, Athens, Ohio 45701, USA
[4] North Carolina State University, Raleigh, NC 27695, USA
[5] Institute of Isotope and Surface Chemistry, Chemical Research Centre HAS, Budapest, Hungary
[6] Department of Physics, University of Oslo, N-0316 Oslo, Norway
[7] San Diego State University, San Diego, CA 92182, USA

Recieved: 02 December 2005 ; **Revised:** 03 April 2006 **Accepted:** 04 July 2006

1. INTRODUCTION

Understanding nuclear level densities and radiative strength functions (RSFs) is important for pure and applied nuclear physics. The Oslo group has developed a method, the so called Oslo method, to extract both the level density and the radiative strength function simultaneously from primary γ spectra after a light-ion reaction (Schiller et al., 2000). The method has been applied to study several rare-earth isotopes which are deformed and have high level densities. The method works well for heavy nuclei. As an extension of the method to a lighter mass region we study ^{56,57}Fe and to a medium mass region we study ^{96,97}Mo isotopes. The iron isotopes are of particular interest since they are the seed nuclei for the synthesis of the heavy elements by the *s* and *r* processes. The nucleus ^{96}Mo is of special interest in the investigation of the |N-Z| dependence of level densities, since A=96 isobars are the only ones in the nuclear chart where one can find three different stable nuclei with |N-Z| varying by eight units from ^{96}Zr to ^{96}Ru.

2. EXPERIMENTAL DETAILS

The experiment was carried out with a ~ 2-nA beam of 45-MeV ^{3}He particles at the Oslo Cyclotron Laboratory. The self supporting targets ^{57}Fe and ^{97}Mo were enriched to 94.7 % and 94.2 % and had 3.4-mg/cm^2 and 2.1 mg/cm^2 thicknesses, respectively. Each experiment ran for ~ 5 days, and 200,000 particle-γ coincidences were recorded in (^{3}He,αγ) and (^{3}He,^{3}He'γ) reaction channels. The outgoing charged particles were detected and their energies were measured by eight collimated Si ΔE-E telescopes, placed 5 cm from the target in a ring, 45° with respect to the beam direction. The thicknesses of the front and end detectors were 140 and 3000 μm, respectively. The total solid angle coverage was 0.3 % of 4π, and the energy resolution was ~ 0.3 MeV over the entire spectrum. The γ rays were measured by 28 collimated 5"x5" NaI(Tl) detectors surrounding the target and the particle detectors. The total efficiency was 15% of 4π and the energy resolution was 6 % of the deposited energy at 1.3 MeV. In addition, one 60 % HPGe detector was used in order to monitor the selectivity and populated spin distribution of the reactions.

From the known Q value and the reaction kinematics, the particle energy is converted into the initial excitation energy of the residual nucleus. A γ-ray spectrum for each excitation energy bin was constructed from the coincidence data. These spectra were then unfolded using the detector response functions in order to eliminate incomplete energy contributions (Guttormsen et al., 1996). The primary γ spectrum for each excitation energy bin was then extracted using a subtraction method (Guttormsen et al., 1987). The basic assumption underlying this method is that the γ decay pattern from any excitation energy bin is independent of the population mechanism of the states within the bin. In Figure 1, raw, unfolded, and primary γ-ray spectra are shown for the ^{57}Fe (^{3}He,αγ) ^{56}Fe and ^{57}Fe (^{3}He,^{3}He'γ) ^{57}Fe reactions.

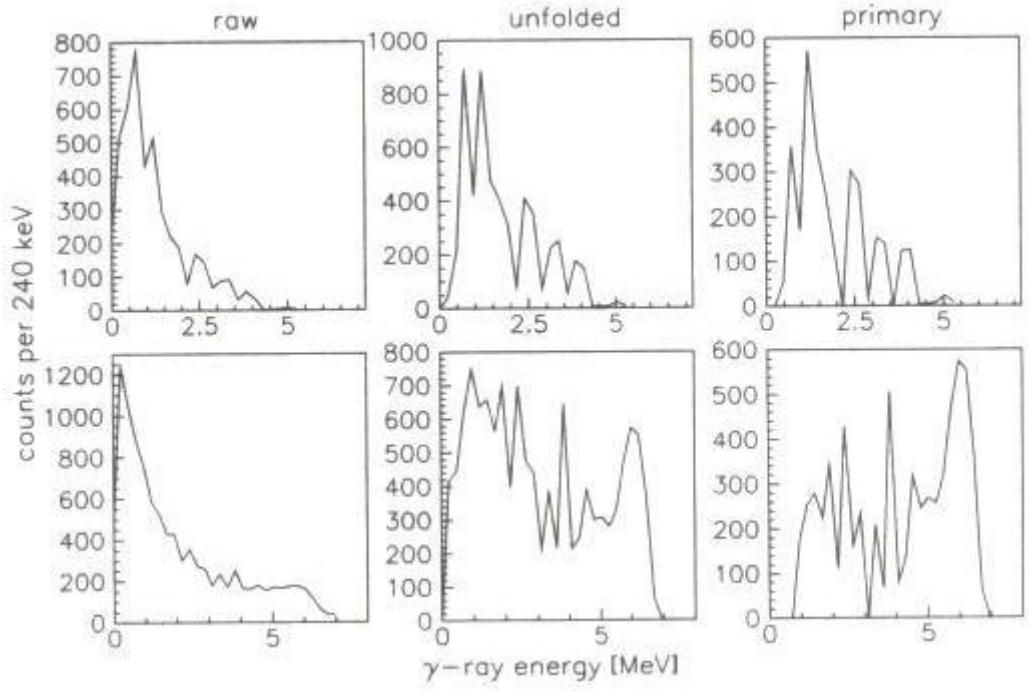

Figure 1. Raw, unfolded, and primary γ spectra from the ^{57}Fe(^{3}He, αγ) ^{56}Fe reaction at 5MeV excitation energy (upper panels) and from the ^{57}Fe(^{3}He, ^{3}He'γ) ^{57}Fe reaction at 6.2 MeV excitation energy (lower panels).

3. METHOD

The experimental primary γ matrix $P(E,E_\gamma)$ is the starting place to extract the level density and the γ–ray strength function. This matrix is factorized into a γ–ray transmission coefficient $T(E_\gamma)$, which depends only on the γ–ray energy, and the level density at the final level $\rho(E_f)$ using the Brink-Axel hypothesis (Brink, 1955), according to which the giant dipole resonance (GDR) can be built on every excited state and the width of the GDR does not depend on the temperature of the state on which it was built. Here this hypothesis is generalized to include any type of nuclear excitation as well as the GDR:

$$P(E,E_\gamma) \propto T(E_\gamma)\rho(E-E_\gamma) \quad \textbf{(1)}$$

where E is the initial excitation energy. The functions T and ρ are extracted by a least χ^2 fit to the primary γ spectra using no *a priori* assumption for the functional form of either the level density or the γ–ray transmission coefficient (Schiller *et al.*, 2000). The agreement between the experimental primary γ-ray spectrum and the least χ^2 fit is very good as shown in Figure 2. Due to the functional form of Eq. (1) there are an infinite number of solutions. All of these solutions are related to each other by the following equations if one solution is known (Schiller *et al.*, 2000) :

$$\begin{aligned}\tilde{\rho}(E-E_\gamma) &= A\exp\left[\alpha(E-E_\gamma)\right]\rho(E-E_\gamma)\\ \tilde{T}(E_\gamma) &= B\exp\left(\alpha E_\gamma\right)T(E_\gamma)\end{aligned} \quad \textbf{(2)}$$

The least χ^2 fit provides one of the solutions. The most relevant solution is then obtained by determining the free parameters A, B, and α using independent experimental information. The number of discrete levels at low excitation energy (Firestone and Shirley, 1996) and the average neutron resonance spacing at the binding energy B_n are used to determine the parameters A and α. The parameters B is then determined using the average total radiative width of neutron resonances assuming that the main contribution to the radiative strength comes from dipole transitions (Voinov et al., 2001). The normalization procedure is well determined for the ^{57}Fe. Unfortunately, there are no experimental (n,γ) data for ^{56}Fe. Therefore the level density for ^{56}Fe is normalized using information from the neighboring ^{57}Fe isotope. A normalization factor is determined by comparing the known level density at B_n with the one obtained from the Fermi-gas model in ^{57}Fe according to the von Egidy parameterization (von Egidy et al., 1988). This factor is then multiplied by the Fermi-gas level density of ^{56}Fe with the appropriate von Egidy parameterization, which is then employed in the normalization. We proceed the same way for the Mo isotopes.

4. LEVEL DENSITIES

Normalized level densities for ^{56,57}Fe and ^{96,97}Mo are shown in Figure 3. A prominent feature in the level density curves is the step structure at low excitations. The steps at 2.9 MeV in ^{56}Fe and 1.8 MeV in ^{57}Fe are also supported by the data obtained from the counting of discrete levels. However, the discrete-level data cannot follow the experimental level density due to the missing levels at high excitation energy. The steps are less pronounced in Mo isotopes. The step at 1.5 MeV in ^{97}Mo cannot be observed from the counting of discrete levels due to the high level density. The step structure at low excitations is interpreted as the breaking of the Cooper pairs. The pairing energy, which is related to the excitation energy difference of the first steps between the two neighboring isotopes, can be calculated using the three-mass indicator of (Dobaczewski et. al.,2001). This calculation yields 1.3 MeV for the Fe, and 1.1 MeV for the Mo nuclei which agree well with the experimental excitation energy differences.

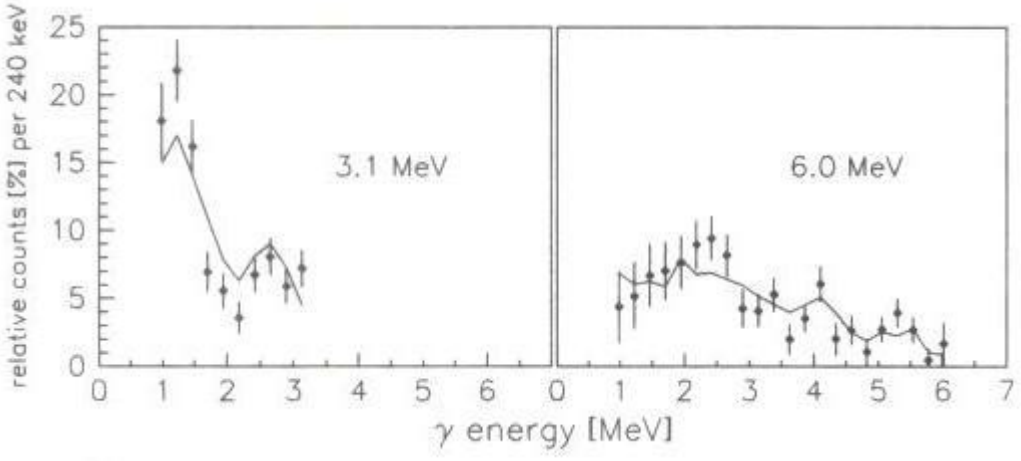

Figure 2. Experimental primary γ spectra (data points with error bars) at two different initial excitation energies (Ex = 3.1 MeV and Ex = 6.0 MeV) compared to the least χ^2 fit (solid lines) for the ^{97}Mo(^{3}He, ^{3}He'γ) ^{97}Mo reaction.

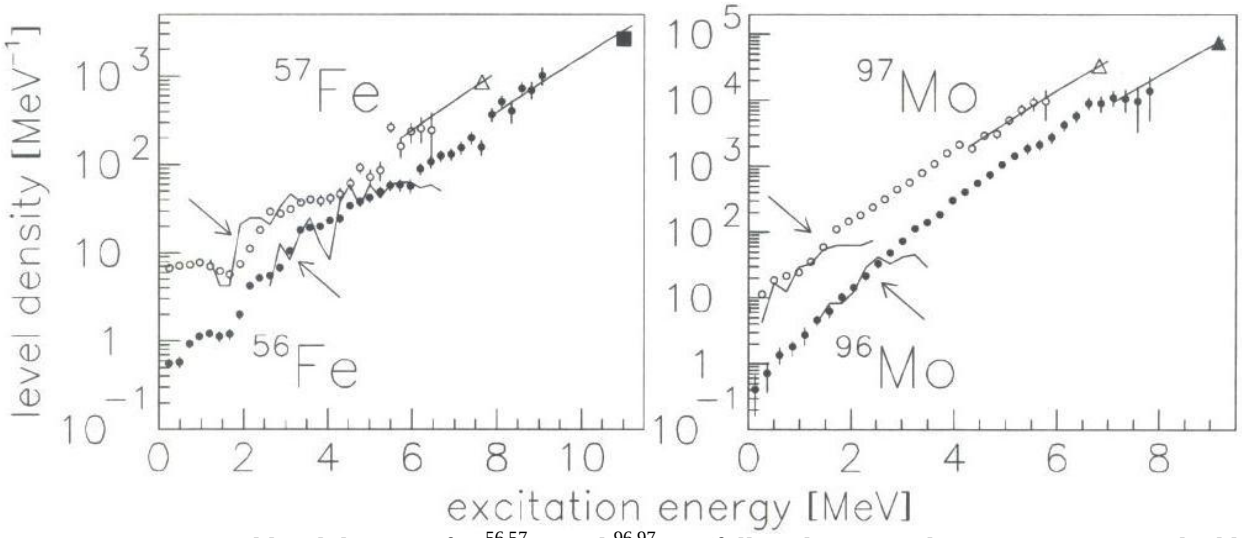

Figure 3. Experimental level densities for ^{56,57}Fe and ^{96,97}Mo (full and open circles represent even and odd nuclei, respectively). The triangles and the square represent the level density data from neutron resonance spacing, and from a particle evaporation study, respectively. The smooth solid curves are the renormalized level density parameterizations according to (von Egidy et al., 1988). The jagged solid lines are the level density information from counting of discrete levels (Firestone and Shirley, 1996). Apparent step structures in the level densities are marked by arrows. In the level density of ^{56}Fe, the bump and the plateau at 0.8 MeV and 2.0 MeV, respectively, are due to the first and second excited states (Schiller et al., 2003).

The proton pairing energies are also calculated using the three-mass indicator of (Dobaczewski et. al.,2001) which gives 0.7 MeV and 1.0 MeV for the Fe and Mo nuclei, respectively, which should give the excitation energies of the first steps in the two odd nuclei. However, the experimental excitation energies are 1.8 MeV (^{57}Fe) and 1.2 MeV (^{97}Mo) which are, respectively, 1.1 MeV and 0.2 MeV higher than the estimates of the three-mass indicator. This can be explained as follows: In order to break one pair and excite one of the nucleons into the lowest unoccupied single-particle state, an energy on the order of the single particle energy is required in addition to the pairing energy. Calculated average spacings (1.9 MeV for ^{57}Fe and 1.3 MeV for ^{97}Mo) explain the higher excitation energy for the appearance of the step structure in ^{57}Fe compared to ^{97}Mo.

Here we also investigate the smooth step structures using a simple model with a Hamiltonian in the following form (Schiller *et al.*, 2003).

$$\hat{H} = \varepsilon \sum_{i=1}^{8} i a_i^{+} a_i - \frac{1}{2} G \sum_{i,j=1}^{8} a_i^{+} a_{\bar{i}}^{+} a_{\bar{j}} a_j - \frac{1}{2} \kappa \sum_{i,j,k,l=1}^{8} W_{ijkl} a_i^{+} a_j^{+} a_k a_l \qquad \textbf{(3)}$$

where a^+ and a are fermion creation and annihilation operators and the labels with bars indicate time reversed orbits. The parameters ε, G, and κ are the single-particle level spacing, the strength of the pairing interaction, and the strength of the seniority-nonconserving interaction W, respectively. In the case where the seniority is conserved, i.e. $\kappa = 0$, the level density looks as the dotted line in Figure 4. The separated distributions correspond to levels with the same seniority. The number of levels increases as the

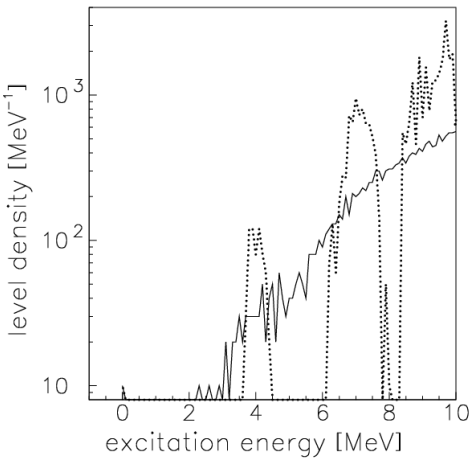

Figure 4. Level density as a function of excitation energy. Model calculation (dotted line) using the Hamiltonian of Eq. (3) with ε = 0.25 MeV, G = 0.5 MeV, and $\kappa \approx 0$ MeV. Adding a random two-body interaction with the strength κ = 0.14 MeV (solid line) results in a step structure similar to the one in the experimental level density of Fe isotopes (Schiller et al., 2003).

seniority increases, which shows that the step structures in the level density can be explained by the breaking of nucleon pairs. In order to obtain smooth steps as in the case of the experimental level density curves, one must include the seniority non-conserving term in the Hamiltonian, i.e. $\kappa \neq 0$. For simplicity we choose to model seniority non-conserving interaction by a random two-body interaction (Mon and French, 1975). For the present calculation we used ε = 0.25, G = 0.5 MeV, and κ =

0.14 MeV. The level density obtained from this calculation is shown in Figure 4 on the top of the level density with pure pairing. The gaps between the bumps are rapidly filled giving a smooth step structure as observed in the experimental level densities. The choice of the strength of the random interaction changes the structure of the level density significantly. The range between κ = 0.13 MeV and κ = 0.16 MeV gives the best qualitative agreement with the Fe data. A much stronger random interaction ($\kappa \geq$ 0.2 MeV) produces a more smeared out step structure in the level density curve similar to the Mo data.

5. RADIATIVE STRENGTH FUNCTIONS

The normalized RSFs for ^{56,57}Fe and ^{96,97}Mo using the average total radiative width ‹Γγ› as described in (Voinov et al., 2001) are shown in Figure 5 and Figure 6, respectively. In the normalization procedure, we assume (i) equal number of positive and negative parity states at any energy below neutron separation energy, and (ii) only *E1* and *M1* dipole contribution to the photon strength. The unusual feature of the RSFs for all nuclei is a large strength for soft transitions ($E_\gamma \leq$ 4 MeV for Fe isotopes and $E_\gamma \leq$ 3 MeV for Mo isotopes). This enhancement has not been observed in the rare-earth nuclei. Theoretical models cannot produce the present soft γ strength. Although KMF model takes into account the temperature dependence of the RSF, it is insufficient to describe the data.

We investigated the RSFs of $^{93\text{-}98}$Mo isotopes using the (^{3}He,αγ) and (^{3}He,^{3}He'γ) reactions in a recent paper (Guttormsen et al., 2005). In Figure 6, we show results of ^{96}Mo and ^{97}Mo isotopes obtained from these two reactions. Both types of the reactions give very similar RSFs.

In the lower panels of Figure 5, we plot the RSFs for different excitation energy windows; thus, show that the shape of the RSFs does not depend on the excitation energy. As a phenomenological approach we describe the experimental RSFs as a sum of a KMF model for *E1* strength, Lorentzian descriptions of the GMDR, isoscalar *E2* resonance, and a power law modeling the large enhancement at low energies:

$$f_\Sigma = K\left(f_{E1} + f_{M1} + \frac{A}{3\pi^2 c^2 \hbar^2} E_\gamma^{-B} \right) + E_\gamma^2 f_{E2} \qquad \textbf{(4)}$$

The parameters of the RSF models are taken from systematics (Oblozinsky, 1998). The fit parameters *K*, *A*, and *B* for five reactions are given in Table.1.

We also investigated the RSF with a different method, i.e. TSC method ^{56}Fe(n,2γ)^{57}Fe, in order to show that the soft enhancement is independent of the experimental method. The TSC measurement is based on multiplicity-two events populating the low-lying levels after the thermal neutron capture. Following the neutron capture, the nucleus decays into the ground state or one of the low-lying levels by two subsequent γ rays. The sequence of these first and second γ rays is unknown experimentally. However, the fact that the discrete levels are experimentally resolvable enables one to separate soft primary and soft secondary transitions. Once these individual peaks are subtracted from the spectrum, the remaining continuous spectrum is the contribution from the soft primary γ transitions. The details of the experiment, the analysis procedure, and the TSC method can be found elsewhere (Voinov et al., 2004). Figure 7 shows the intensity of the soft primary γ transitions (data points).

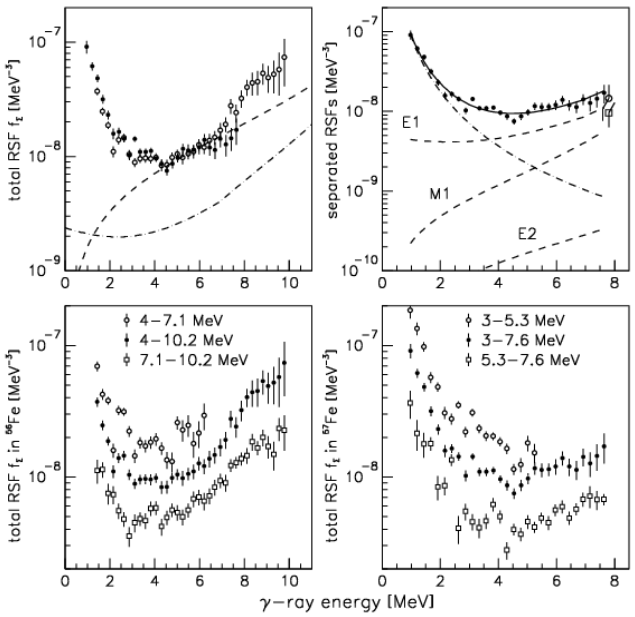

Figure 5. Upper left panel: Total RSF f∑ of ^{56,57}Fe (solid and open circles, respectively); Lorentzian (dashed line) and KMF model (dashed-dotted line) descriptions of the GEDR. Upper right panel: Fit (solid line) to ^{57}Fe data and decomposition into the renormalized E1 KMF model, Lorentzian *M1* and *E2* models (all dashed lines), and a power law to model the large enhancement for low energies (dash-dotted line). Open symbols are estimates of the *E1* (circle) and *M1* (square) RSF from hard primary γ rays. Lower panels: Total RSF in ^{56}Fe (left) and ^{57}Fe (right) for different excitation energy windows (Voinov et al., 2004).

Now one can calculate the intensity of the ordered TSCs between an initial and final state using the statistical model of the γ decay from compound states:

$$I_{if}(E_1, E_2) = \sum_{XL, XL', J_m^\pi} \frac{\Gamma_{im}^{XL}(E_1)}{\Gamma_i} \rho(E_m, J_m^\pi) \frac{\Gamma_{mf}^{XL'}(E_2)}{\Gamma_m} \qquad \textbf{(5)}$$

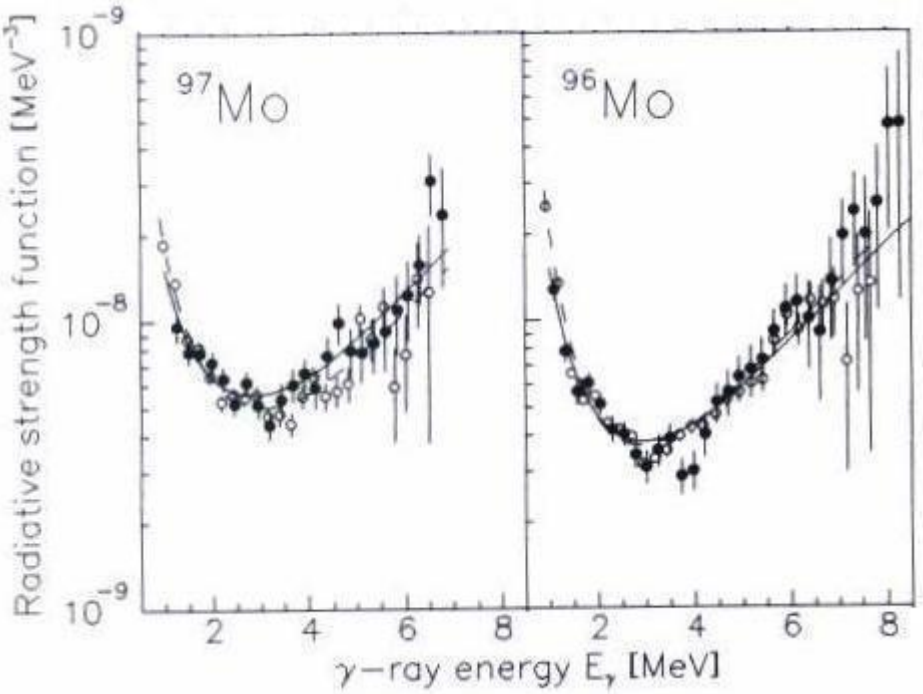

Figure 6. Normalized RSFs for ^{96,97}Mo (Guttormsen et al., 2005). The filled and open circles represent data taken with the (^{3}He, α) and (^{3}He, ^{3}He') reactions, respectively. The solid and dashed lines are fits to the RSF data from the two respective reactions (see text).

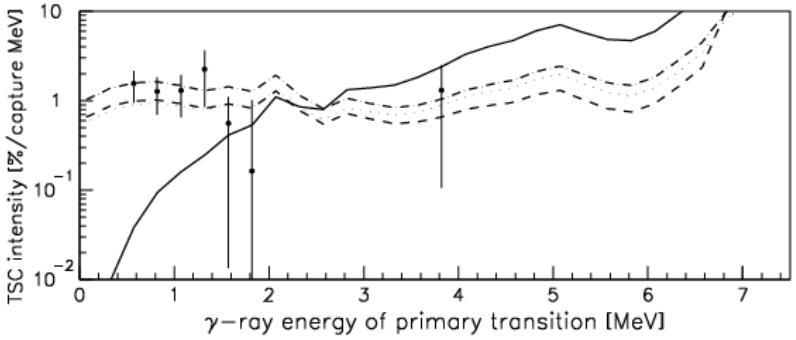

Figure 7. Experimental TSC intensities (compressed to 250-keV-broad γ energy bins) for cascades with soft primary γ rays and at the midpoint of the spectrum (data points with error bars). Lines are statistical-model calculations based on experimental data for the level density and f_Σ, neglecting (solid line) and assuming E1 (dashed line), M1 (dash-dotted line), and E2 (dotted line) multipolarity for the soft pole of the RSF.

Table1. Fitting parameters of Eq. (4) for different reactions.

Reaction	*K*	*A* (mb/MeV)	*B*
^{57}Fe(^{3}He,^{3}He')^{57}Fe	2.1(2)	0.47(7)	2.3(2)
^{96}Mo(^{3}He,^{3}He')^{96}Mo	0.36(1)	0.60(4)	3.2(2)
^{97}Mo(^{3}He,α)^{96}Mo	0.32(4)	0.47(14)	2.7(6)
^{97}Mo(^{3}He,^{3}He')^{97}Mo	0.38(3)	0.47(7)	2.4(3)
^{98}Mo(^{3}He,α)^{97}Mo	0.45(5)	0.30(10)	2.2(5)

where E_1 and E_2 are the energies of the first and the second transitions in the TSC which are connected by $E_i - E_f = E_1 + E_2$. Γ_{im} and Γ_{mf} are partial decay widths and Γ_i and Γ_m are total decay widths of the initial and intermediate levels, respectively. The average values of these widths are calculated using

$$\Gamma_{if}^{XL}(E_\gamma) = \frac{f_{XL}(E_\gamma)E_\gamma^{2L+1}}{\rho(E_i, J_i^\pi)} \quad \textbf{(6)}$$

where f_{XL} is the RSF for a transition with multipolarity XL and energy E_γ, and $\rho(E_i,J_i^\pi)$ is the level density for initial states i at energy E_i with equal spin and parity J_i^π. In Eq. (6), we use the data for level density and RSF from the Oslo experiment. The

calculations were performed first by neglecting the soft pole, i.e. third term in Eq. (4), and then by assuming *E1*, *M1*, and *E2* multipolarity for the soft pole. It is clear that the calculation without the soft pole cannot reproduce the TSC data (see Figure 7). The other assumptions of *E1*, *M1*, and *E2* multipolarity for the soft pole make no difference within the experimental uncertainty, thus, the multipolarity of the soft pole remains unknown.

6. CONCLUSION

Nuclear level densities and radiative strength functions in ^{56,57}Fe and ^{96,97}Mo are extracted experimentally from primary γ-ray spectra. The present study and the study of several other nuclei, including Si, other Mo isotopes, and many rare-earth nuclei, have shown that the statistical Oslo method works well in all of these mass regions. The most interesting finding in the level density is the step structure, which is interpreted as the breaking of the Cooper pairs in the nucleus. A simple microscopic model with a Hamiltonian, which includes pairing, seniority-conserving, and seniority-nonconserving interaction terms, can qualitatively produce a similar step structure observed in the experimental data for the strength of the seniority-nonconserving interaction parameter κ = 0.14 MeV for the Fe isotopes. The smoothness of the step structure in the level density of the Mo isotopes indicates a stronger seniority-nonconserving interaction for these nuclei. The RSFs for all nuclei show an unusual enhancement at low γ energies. This effect cannot be explained by the current phenomenological models. The total RSF can be described by a KMF model for *E1* radiation, Lorentzian models for *M1* and *E2* radiations, and a power law to model the soft pole. In a completely different experiment using the ^{56}Fe(n,2γ) reaction, the two-step cascade intensities of soft primary transitions are measured. Statistical model calculations based on the level density and RSF from the Oslo experiment reproduce the experimental TSC intensities only in the presence of the soft pole in the total RSF.

Part of this work was performed under the auspices of the U.S. Department of Energy by the University of California, Lawrence Livermore National Laboratory under Contract No. W-7405-ENG-48. Financial support from the Norwegian Research Council (NFR) is gratefully acknowledged. Part of this work was supported by the EU5 Framework Programme under Contract No. HPRI-CT-1999-00099. G.M., U.A., and E.A. acknowledge support by U.S. Department of Energy Grant No. DE-FG02-97-ER41042. Part of this research was sponsored by the National Nuclear Security Administration under the Stewardship Science Academic Alliances program through DOE Research Grants No. DE-FG03-03-NA00074 and No. DE-FG03-03-NA00076.

7. REFERENCES

Brink, D.M. (1955), Ph.D. thesis, Oxford University; Axel, P. (1962). *Phys. Rev.* 126, 671.

Dobaczewski, J., Magierski, P., Nazarewicz, W., Satula, W., and Szymanski, Z. (2001). *Phys. Rev.* 63(C), 024308.

Firestone, R.B. and Shirley, V.S. (1996). Table of Isotopes, 8th ed. (Wiley, New York), Vol II.

Guttormsen, M., Chankova, R., Agvaanluvsan, U., Algin, E., Bernstein, L.A., Ingebretsen, F., Lönnroth, T., Messelt, S., Mitchell, G.E., Rekstad, J., Schiller, A., and Siem, S., Sunde, A.C., Voinov, A., Odegard, S. (2005). *Phys. Rev.* 71(C), 044307.

Guttormsen, M., Ramsoy, T., and Rekstad, J. (1987). *Nucl. Instrum. Methods Phys. Res*. 255(A), 518.

Guttormsen, M., Tveter, T.S., Bergholt, L., Ingebretsen, F., and Rekstad, J. (1996). *Nucl. Instrum. Methods Phys. Res.* 374(A), 371.

Mon, K.K. and French, J.B. (1975). *Ann. Phys. (N.Y)* 95, 90.

Oblozinsky, P. (1998). IAEA Report No. IAEA-TECDOC-1034.

Schiller, A., Algin, E., Bernstein, L.A., Garrett, P.E., Guttormsen, M., Hjorth-Jensen, M., Johnson, C.W., Mitchell, G.E., Rekstad, J., Siem, S., Voinov, A., Younes, W. (2003). *Phys. Rev.* 68(C), 054326.

Schiller, A., Bergholt, L., Guttormsen, M., Melby, E., Rekstad, J., and Siem, S. (2000). *Nucl. Instrum. Methods Phys. Res.* 447(A), 498.

Voinov, A., Algin, E., Agvaanluvsan, U., Belgya, T., Chankova, R., Guttormsen, M., Mitchell, G.E., Rekstad, J., Schiller, A., and Siem, S. (2004). *Phys. Rev. Lett.* 93, 142504.

Voinov, A., Guttormsen, M., Melby, E., Rekstad, J., Schiller, A., and Siem, S. (2001). *Phys. Rev.* 63(C), 044313.

von Egidy, T., Schmidt, H.H., and Bekhami, A.N. (1988). *Nucl. Phys*. 481(A), 189.